4-Nitroanisole Facilitates Proton Reduction: Visible Light-Induced Oxidative Aryltrifluoromethylation of Alkenes with Hydrogen Evolution

Rui Kong,[a] Tingfeng Fu,[a] Ruihan Yang,[a] Danna Chen,[a] Deqiang Liang,*[a] Ying Dong,[b] Weili Li,[a] and Baoling Wang[a]

A complementary oxidative photocatalytic strategy is presented. In the presence of 4-nitroanisole, hexafluoroisopropanol (HFIP) as a proton source is activated and the proton photoreduction is enhanced, enabling a range of cyclizative aryltrifluoromethylations of alkenes and CF_3SO_2Na (Langlois' reagent) with hydrogen evolution. Such a protocol is general, for both activated and unactivated olefins could be used as the substrates, affording a variety of CF_3-containing heterocycles such as indolines, indolin-2-ones, 3,4-dihydroisoquinolin-1-ones, 5,6-dihydrobenzoimidazo[2,1-*a*]isoquinolines, benzoimidazo[2,1-*a*]isoquinolin-6(5*H*)-ones and 1,2,3,4-tetrahydroisoquinolines, under mild and metal- and oxidant-free conditions with a good functional-group tolerance. Extensive mechanistic investigations revealed that *p*-nitroanisole (*p*-NA) does not react with the photocatalyst directly as an oxidant, but rather activates HFIP via proton-coupled electron transfer (PCET) and scavenges some of the reduced protons to improve proton photoreduction.

Introduction

Stimulated by the growing global concern regarding sustainability,[1] photoredox catalysis, which is usually mild and green, emerged in recent years as a potent synthetic tool to effect redox event and access molecular complexity.[2] By taking advantage of visible light as an energy input, such a technique is of particular power in redox-neutral syntheses.[3] Net-oxidative[4] or -reductive transformations[5] could be achieved as well by incorporating a terminal oxidant and reductant, respectively, into the photocatalytic cycle, albeit with additional chemical wastes. From the point of view of minimal waste, using the proton as an innocuous sacrifice to accept an electron, which is a common practice in electrochemical oxidation,[6] to achieve photooxidation with hydrogen as the sole byproduct, is an appealing and ideal concept. Nevertheless, oxidative photocatalysis with hydrogen evolution to give value-added organic molecules remains a formidable challenge, and such examples are rare.[7] A visible-light photon (400–700 nm) possesses an energy of only 1.8–3.1 eV, and it is further diminished via intersystem crossing or nonradiative pathways,[8] rendering the excited state of a photosensitizer usually not reducing enough to release an electron to the proton efficiently. The combination of, say, a cobaloxime co-catalyst might improve the efficiency of proton reduction to allow matched oxidation and H_2 production rates (Scheme 1a),[9,10] and some oxidative transformations were achieved by merging photocatalysis with electrochemistry (Scheme 1b).[11,12] We wish to communicate a complementary oxidative photosynthetic strategy with hydrogen evolution, wherein the proton reduction efficiency is improved by activating the proton source of hexafluoroisopropanol (HFIP) with *p*-nitroanisole[13] (*p*-NA) via proton-coupled electron transfer (PCET, Scheme 1c).[14]

Organofluorine compounds exhibit improved biological, physical, and chemical properties compared to those of their C–H counterparts, and combining several biologically active segments in one molecule is a cornerstone of pharmaceutical research and drug development.[15] In this regard, cyclizative aryltrifluoromethylation of alkenes is a reliable protocol to construct CF_3-containing carbo-/heterocycles.[16] Existing methods fall into three categories: (a) Redox-neutral cyclizations using highly reactive CF_3SO_2Cl,[17] gaseous CF_3I[18] or other elaborated CF_3 sources bearing an atom-uneconomic leaving group (LG),[19] induced by visible light or heat and/or catalyzed by a noble metal (Scheme 2a). (b) Oxidative aryltrifluoromethylation of, say, Togni reagent,[20] $PhICF_3Cl$,[21] CF_3SO_2Na[22] or Me_3SiCF_3,[23] mediated by a stoichiometric excess of an external

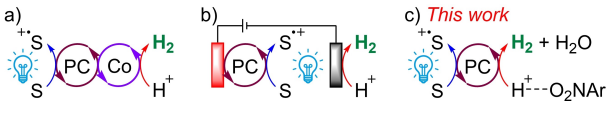

Scheme 1. Oxidative photocatalysis with hydrogen evolution.

[a] R. Kong, T. Fu, R. Yang, D. Chen, Prof. Dr. D. Liang, Prof. W. Li, Prof. Dr. B. Wang
School of Chemistry and Chemical Engineering
Kunming University
2 Puxin Road, Kunming, Yunnan Province,
650214, Kunming, (P. R. China)
E-mail: liangdq695@nenu.edu.cn
ldq@kmu.edu.cn
[b] Dr. Y. Dong
College of Chemistry,
Chemical Engineering and Materials Science
Shandong Normal University
Jinan, Shandong Province,
250014 (P. R. China)

Supporting information for this article is available on the WWW under https://doi.org/10.1002/cctc.202100304

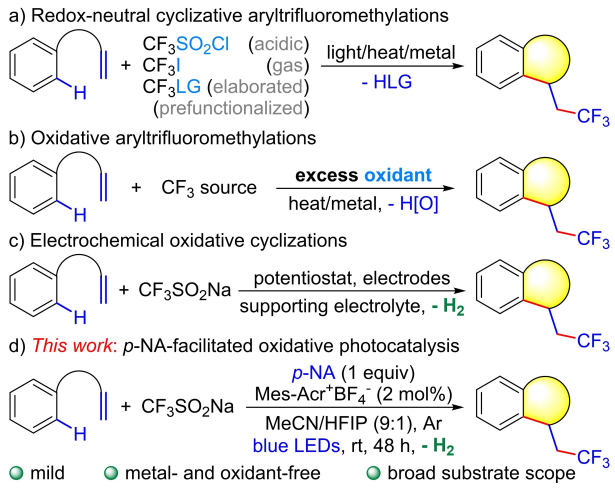

Scheme 2. Cyclizative aryltrifluoromethylations of alkenes.

oxidant often enough at an evaluated temperature and/or in the presence of a metal catalyst (Scheme 2b).[24] (c) Electrochemical oxidation with hydrogen evolution performed with expensive electrodes and specialized electrochemical apparatuses in the presence of large amounts of supporting electrolyte (Scheme 2c).[25] Among these, reactions involving CF_3SO_2Na, a neutral, benchtop-stable and inexpensive solid termed as Langlois' reagent,[26] are the most attractive, yet they need to be carried out under oxidizing conditions using either an oxidant[22] or an anode.[25] He, Guan and co-workers reported an oxidative photosynthesis of sulfonyl-containing isoquinolinediones with hydrogen evolution from activated alkenes and sodium sulfinate, but with CF_3SO_2Na as the radical precursor the corresponding trifluoromethylated product was obtained in only a poor yield of 37%.[27] As part of our ongoing interest in green radical chemistry,[28] herein we report a visible light-induced oxidative aryltrifluoromethylation of CF_3SO_2Na with a range of alkenes under mild and exogenous oxidant-free conditions (Scheme 2d). HFIP serves as the proton source to produce hydrogen, and *p*-NA is used to activate HFIP and scavenge some of the reduced protons to improve proton photoreduction. Such an electrochemistry-like methodology is practical and general, and both activated and unactivated olefins could be used as the substrates, affording a variety of CF_3-containing heterocycles such as indolines, indolin-2-ones, 3,4-dihydroisoquinolin-1-ones, 5,6-dihydrobenzoimidazo[2,1-*a*]isoquinolines, benzoimidazo[2,1-*a*]isoquinolin-6(5*H*)-ones and 1,2,3,4-tetrahydroisoquinolines. The mild oxidizing environment contributes to a good functional group tolerance.

Results and Discussion

We began our investigation using an unactivated alkene of *N*-(2-methylallyl)-*N*-phenylacetamide **1a** as the model substrate (Table 1; see the Supporting Information for full details). In the presence of 1 mol% of Mes-Acr$^+$BF$_4^-$ and 2 equiv. of CF_3SO_2Na

Table 1. Optimization of reaction conditions.

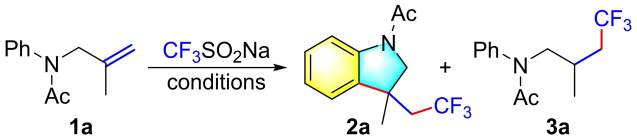

1a **2a** **3a**

Entry	Conditions[a]	2a/3a [%][b]
1	Mes-Acr$^+$BF$_4^-$ (1 mol%), CF_3SO_2Na (2 equiv), MeCN/HFIP (4:1, 10 mL), blue LEDs, Ar, rt, 24 h	34/11
2	entry 1 but CH_3CN as the solvent	19/5
3	entry 1 but HFIP as the solvent	15/8
4	entry 1 but MeCN/MeOH (4:1) as the solvent	16/5
5	entry 1 but 4CzIPN as the PC	26/13
6	entry 1 but Ir(ppy)$_3$ as the PC	trace/–
7	entry 1 and Co(dmgH)$_2$PyCl (3 mol%)	nr/–
8	entry 1 and CCE = 2 mA[c]	5/1
9	entry 1 but at 50 °C	36/–
10	entry 1 but under air	trace/–
11	entry 1 and $K_2S_2O_8$ (0.5 equiv)	28/5
12	entry 1 and $PhNO_2$ (1 equiv)	30/4
13	entry 1 and *p*-DNB (1 equiv)	trace/–
14	entry 1 and *p*-NA (1 equiv)	51/–
15	entry 14 but Mes-Acr$^+$BF$_4^-$ (2 mol%), MeCN/HFIP (9:1, 5 mL), 48 h	60/–

[a] Reaction conditions: **1a** (0.5 mmol), CF_3SO_2Na (2.0 equiv), Mes-Acr$^+$BF$_4^-$ (2 mol%), *p*-NA (1.0 equiv), MeCN/HFIP (9:1, v/v, 5.0 mL), 6 W blue LEDs, Ar, room temperature, 48 h. [b] **2a** and **3a**, possessing similar polarities, were collected together by column chromatography, and subjected to ^{1}H NMR analysis to determine the ratio. **3a** was detected by GC-MS analysis, and the pure product of **3b**, a derivative of **3a** bearing an acetyl group on the phenyl ring, was obtained, see Table 2. [c] Undivided cell, carbon cloth anode (15 mm × 15 mm × 0.33 mm, WOS1009, Taiwan CeTech), platinum plate cathode (15 mm × 15 mm × 0.3 mm), nBu$_4$NBF$_4$ (1.0 equiv) as the supporting electrolyte, CCE at 2.0 mA while irradiation.

in MeCN/HFIP (4:1, v/v, 0.05 M) at room temperature under blue light-emitting diode (LED) irradiation for 24 h, **1a** underwent the oxidative trifluoromethylation/cyclization sequence to afford CF_3-containing indolines **2a** with a newly formed quaternary center in 34% yield, along with hydrotrifluoromethylated byproduct **3a** with an *anti*-Markovnikov selectivity in 11% yield (entry 1). We unfortunately failed to isolate any pure product of **3a**, yet its formation was evidenced by the gas chromatography-mass spectrometry (GC-MS) analysis. Furthermore, the pure product of **3b**, a derivative of **3a** bearing an acetyl group on the phenyl ring, was obtained (see Table 2). The use of a pure solvent, such as MeCN (entry 2) or HFIP (entry 3), or of another proton source like MeOH (entry 4) both led to a compromised yield of **2a**. Other photocatalysts (PCs) such as 4CzIPN (entry 5) or Ir(ppy)$_3$ (entry 6) performed worse than Mes-Acr$^+$BF$_4^-$. The formation of the redox-neutral product **3a** suggests that the reaction rate of the proton reduction step of the photocatalytic cycle is low, and thus an efficient oxidative counterpart could not be effected directly. Whilst attempts to improve the reduction efficiency by combining the cobaloxime catalysis (entry 7) or constant current electrolysis (CCE, entry 8) with photocatalysis met with no success, the reaction carried out at an elevated temperature of 50 °C gave **2a** in only a marginally higher yield (entry 9). Whereas the inclusion of air oxidatively degraded substrate **1a** to deliver acetanilide (entry 10), $K_2S_2O_8$ is not an effective terminal oxidant at ambient

Table 2. Photosynthesis of CF_3-containing indolines.[a]

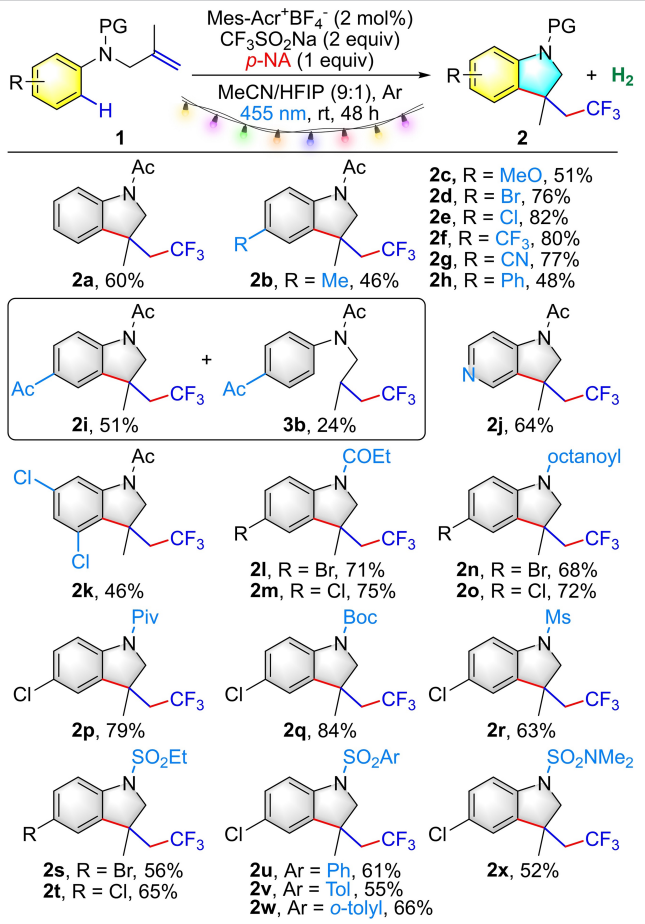

[a] Reaction conditions: **1** (0.5 mmol), CF_3SO_2Na (2.0 equiv), Mes-Acr$^+BF_4^-$ (2 mol%), *p*-NA (1.0 equiv), MeCN/HFIP (9:1, v/v, 5.0 mL), 6 W blue LEDs, Ar, room temperature, 48 h.

temperature (entry 11). Some hydrogen acceptors were evaluated as additives, and the use of nitrobenzene (entry 12) or *p*-dinitrobenzene (*p*-DNB, entry 13) led to inferior results probably due to their ability to inhibit single-electron transfer (SET). To our delight, indoline **2a** was obtained in a better yield of 51% upon addition of *p*-NA (entry 14), with the hydrotrifluoromethylated byproduct **3a** eliminated, suggesting that the efficiency of the proton reduction might be improved. Finally, the yield of indoline **2a** was further improved to 60% using 2 mol% of Mes-Acr$^+BF_4^-$ in MeCN/HFIP (9:1, v/v, 0.1 M, entry 15) for 48 h.

Using proton as an innocuous oxidant, a variety of trifluoromethylated indolines **2** could be prepared under optimized conditions (Table 2). Allylated anilides bearing a methyl, methoxy, bromo, chloro, trifluoromethyl, or cyano group at the *para* position of the *N*-aryl group reacted with Langlois' reagent to give 5-substituted indolines **2b**–**2g** in moderate to high yields. Though both electron-donating and -withdrawing groups were compatible with this transformation, the use of olefins having an electron-deficient *N*-aryl group provided higher yields. *para*-Phenyl-substituted *N*-(2-methylallyl) acetanilide proved to be a challenging substrate, delivering the corresponding trifluoroethyl indoline **2h** in a poor yield. 5-Acetyl indoline **2i** was synthesized from the corresponding 4-acetyl aniline in 51% yield, along with *anti*-Markovnikov hydrotrifluoromethylation byproduct **3b** produced in 24% yield. Notably, the pyridyl functionality was tolerated, and allylated *N*-(pyridin-4-yl) acetamide reacted smoothly to afford 2,3-dihydropyrrolo[3,2-*c*]pyridine **2j** in 64% yield. This protocol might be sensitive to steric factors, and the allyl acetanilide with a 3,5-dichloro group reacted to give the corresponding 4,6-dichloro indoline **2k** in a modest yield.

The scope of the *N*-protecting group (PG) was also investigated. Allylated anilines bearing a propionyl, octanoyl or pivaloyl *N*-PG participated in this cyclization to furnish the related indoline products **2l**–**2p** in good yields. The *tert*-butyloxy-carbonyl (Boc)-protected allyl aniline is a competent substrate as well, furnishing indoline-1-carboxylate **2q** in 84% yield. An evaluation of various sulfonyl PGs revealed that alkylsulfonyl, such as methylsulfonyl and ethylsulfonyl, arylsulfonyl, including phenylsulfonyl, tosyl and *o*-tolylsulfonyl, and *N*,*N*-dimethylsulfamoyl groups, were all tolerated, providing related sulfonyl indolines **2r**–**2x** in moderate yields. Trifluoromethylated small organic molecules are often volatile, and thus some isolated yields might have been damaged during purification.

In an effort to explore the potential of the *p*-NA-facilitated strategy to induce oxidative photocyclization, the title reaction was extended to other alkenes, either unactivated or activated (Table 3). Using an aroyl group as the inbuilt radical trap, *N*-allyl benzamides **4** with a methyl, methoxy or bromo substituent on the aryl ring reacted smoothly with CF_3SO_2Na under optimized reaction conditions, providing CF_3-containing 3,4-dihydroisoquinolin-1-ones **5a**–**5c** in 45–63% yields. *N*-Arylacrylamide **6**, a classic substrate for radical cyclization, also underwent a similar aryltrifluoromethylation to give the desired indolin-2-one product **7**. *N*-Allylated or -acryloylated 2-phenyl benzoimidazoles **8** and **10** are both good performers, providing trifluoromethylated 5,6-dihydrobenzoimidazo[2,1-*a*]isoquinoline **9** or benzoimidazo[2,1-*a*]isoquinolin-6(5*H*)-one **11** in 54% and 48% yields, respectively. The inbuilt radical trapping moiety could be extended to the benzyl group as well, and 1,2,3,4-tetrahydroisoquinoline **13** was successfully prepared from *N*-benzyl allylamine **12**.

It is worthy of notice that a gram-scale synthesis could be readily carried out, and trifluoromethylated indoline **2a** was furnished in only a slightly diminished yield of 56% from 6 mmol of allylated aniline **1a** (Scheme 3), rendering the present protocol highly practical.

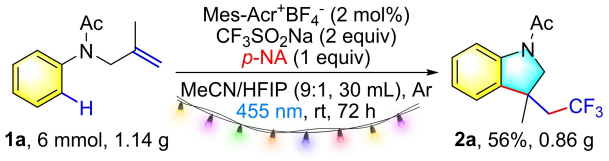

Scheme 3. Gram-scale synthesis.

Table 3. Strategy extension.[a]

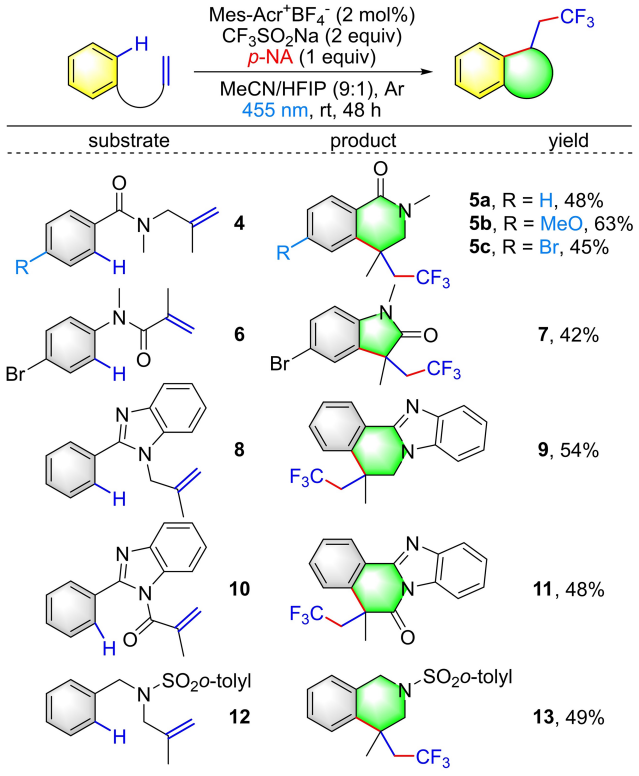

[a] Reaction conditions: **1** (0.5 mmol), CF_3SO_2Na (2.0 equiv), Mes-Acr$^+BF_4^-$ (2 mol%), *p*-NA (1.0 equiv), MeCN/HFIP (9:1, v/v, 5.0 mL), 6 W blue LEDs, Ar, room temperature, 48 h.

In order to ascertain the role of *p*-NA, a range of spectroscopic experiments was carried out. Stern-Volmer quenching studies revealed that the excited state of Mes-Acr$^+$ BF_4^- can be quenched by *p*-NA (Figure 1a), and the quenching effect could be eliminated by introducing large amounts of HFIP (Figures S5–S7). Cyclic voltammetry (CV) tests indicated that *p*-NA has a reduction potential of −1.17 V vs. Ag/AgCl (Figure S19, see the Supporting Information), which is much higher than that of HFIP (−0.86 V vs. Ag/AgCl, Figure S15) and even the solvent MeCN (−0.81 V vs. Ag/AgCl, Figure S16). Furthermore, the reduction waves of *p*-NA disappeared upon inclusion of HFIP, whereas the reduction profile of the MeCN/HFIP mixture (9:1) changed remarkably in the presence of *p*-NA (Figure 1b). It became much steeper, and the current response substantially increased. These data suggest that HFIP might be preferentially reduced over *p*-NA in the reaction, and that the reduction of HFIP could be significantly improved by incorporating *p*-NA. In voltammograms involving small amounts of HFIP (100 μL), while the reduction potentials of HFIP decreased upon inclusion of *p*-NA, a new and stronger reduction peak (−1.02 V vs. Ag/AgCl) was observed (Figures 1c and S22), indicating that there might be a strong non-bonding interaction between the two molecules.[29] Such an interaction was further evidenced by the downfield and hypochromatic shifts observed in the NMR (Figures 1d, S28, and S29) and UV-vis spectra (Figure 1e), respectively, upon mixing HFIP with *p*-NA. Density functional theory (DFT) calculations[30] revealed that HFIP and *p*-NA are hydrogen-bonded, and that other non-bonding interactions are negligible (Figure 1f, see the Supporting Information). Hydrogen detection tests confirmed the hydrogen evolution (Figure 1g), which was somewhat attenuated by adding *p*-NA, suggesting that *p*-NA might scavenge some of the reduced protons probably via PCET to give H_2O and 4-nitrosoanisole.[13,31] The SET from CF_3SO_2Na to the excited PC was also confirmed by Stern-Volmer quenching experiments (Figures 1h, S8–S11).

To probe the radical nature of this transformation, quenching experiments were conducted (Scheme 4a). The model reaction under otherwise optimal conditions was suppressed by doping with either 1 equiv. of 2,2,6,6-tetramethylpiperidine-1-oxyl (TEMPO) or 3 equiv. of 1,1-diphenylethylene (DPE), whereas the use of 5 equiv. of 2,6-di-*tert*-butyl-4-methylphenol (BHT) as the radical scavenger compromised the yield of **2a**. In addition, DPE-CF_3 adduct **14** was detected by ^{19}F NMR analysis in DPE experiment. In the presence of 2 equiv. of a SET inhibitor of *p*-DNB or 1 equiv. of an electron scavenger of $CuCl_2$, the model reaction under standard conditions did not proceed as well. These results indicate that a radical and SET pathway might be involved in this methodology. The kinetic isotope effect (KIE) was determined through parallel experiments with allyl acetamide **1a** and the aryl-deuterated substrate **1a**–d_5 under standard conditions (Scheme 4b), and the minor KIE value of 1.1 indicates that the C–H bond cleavage of the aryl moiety is not the rate-limiting step. The intermittent irradiation experiments showed that the trifluoromethylation/cyclization sequence was fully suppressed in the absence of light (Scheme 4c), thus a constant irradiation is necessary for effective product formation.

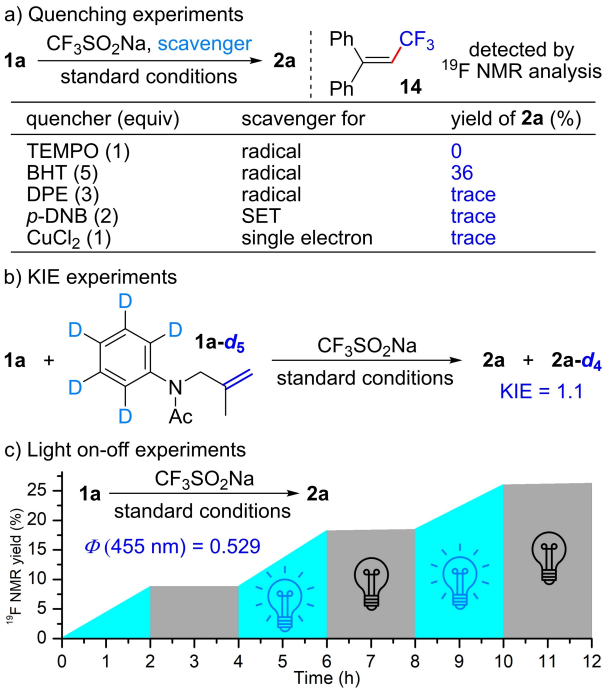

Scheme 4. Further mechanistic investigations.

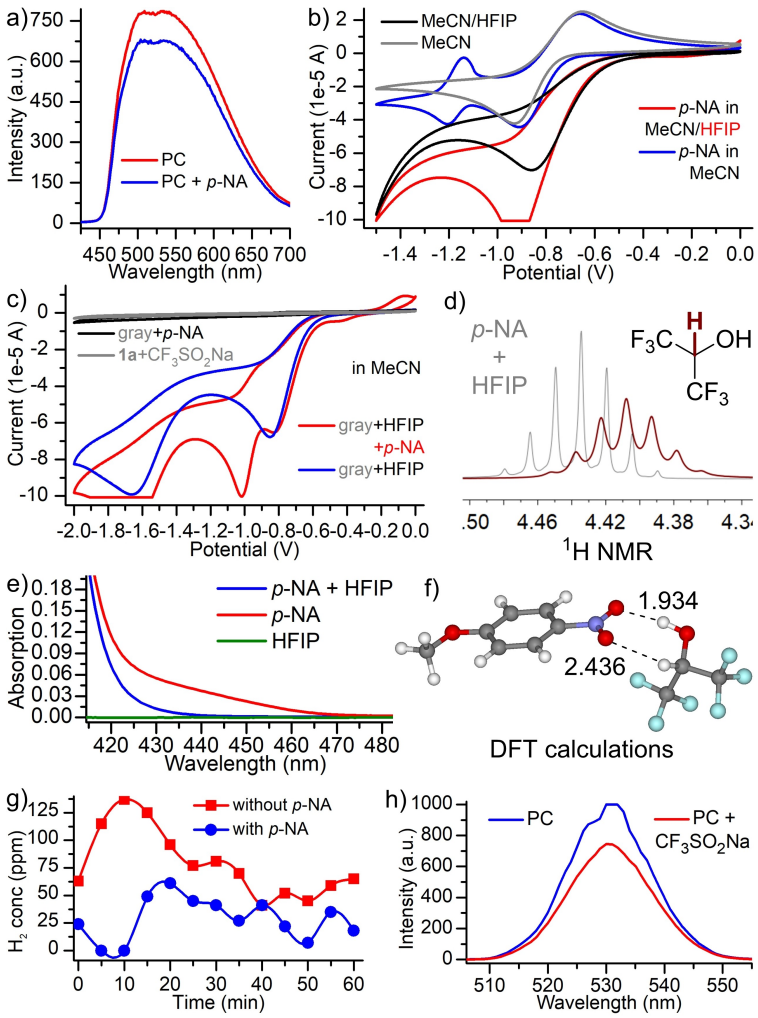

Figure 1. a) Emissions of Mes-Acr$^+$BF$_4^-$ (10^{-3} M) and an equimolar mixture of Mes-Acr$^+$BF$_4^-$ and *p*-NA (10^{-3} M) in MeCN/HFIP (9:1). b) Cyclic voltammograms of *p*-NA (10^{-3} M) in MeCN or MeCN/HFIP (9:1) containing 0.1 M nBu$_4$NBF$_4$. c) Cyclic voltammograms of reaction mixtures in MeCN containing 0.1 M nBu$_4$NBF$_4$. Gray line, **1a** (10^{-3} M) and CF_3SO_2Na (2.0 equiv); black line, **1a** (10^{-3} M), CF_3SO_2Na (2.0 equiv) and *p*-NA (1.0 equiv); blue line, **1a** (10^{-3} M), CF_3SO_2Na (2.0 equiv) and HFIP (100.0 μL); red line, **1a** (10^{-3} M), CF_3SO_2Na (2.0 equiv), HFIP (100.0 μL) and *p*-NA (1.0 equiv). d) ^{1}H NMR spectra of HFIP (0.1 M) and an equimolar mixture of HFIP and *p*-NA (0.1 M) in $CDCl_3$. e) UV-vis spectra of HFIP (0.1 M), *p*-NA (0.1 M), and an equimolar mixture of *p*-NA and HFIP (0.1 M) in MeCN. f) Theoretical calculations of non-bonding interactions between HFIP and *p*-NA. g) Hydrogen detection tests in the absence or presence of *p*-NA (1.0 equiv) using 6 mmol of **1a** under otherwise optimized conditions. h) Fluorescence quenching of Mes-Acr$^+$BF$_4^-$ (10^{-3} M) in the presence of CF_3SO_2Na (5.0 equiv) in petroleum ether.

A quantum yield of 0.529 was determined (see the Supporting Information), and a value below unity suggests that the reaction should proceed by a sequential redox process rather than a radical chain pathway.

On the basis of the observations above, a plausible reaction mechanism is proposed (Scheme 5). Irradiation of the organic dye Mes-Acr$^+$BF$_4^-$ leads to its excited state of Mes-Acr^{+}* with a reduction potential of 1.78 V vs. Ag/AgCl in MeCN/HFIP (9:1) on the basis of electrochemical and spectroscopic measurements (see the Supporting Information), and Mes-Acr^{+}* is oxidizing enough to enable a SET from CF_3SO_2Na (1.32 V vs. Ag/AgCl in MeCN/HFIP (9:1), Figure S13) to afford a molecule of SO_2 and a trifluoromethyl radical ($CF_3^{\bullet}$). The addition of $CF_3^{\bullet}$ to the alkene bond of **1a** delivers alkyl radical **A.** **A** then cyclizes to ring closure intermediate **B** via intramolecular radical tapping by the

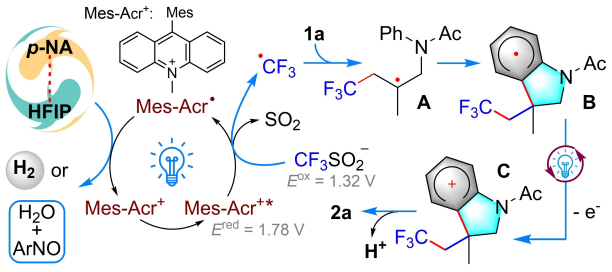

Scheme 5. Proposed mechanism.

aryl group, and the SET from **B** to Mes-Acr^{+}* affords cationic intermediate **C**. Finally, the deprotonation of **C** gives the CF_3-containing indoline **2a**. As for the reduction part of the photocatalytic cycle, HFIP or the complex of HFIP and *p*-NA[29]

reacts with the reduced form of PC (Mes-Acr•) via direct and PCET reduction, respectively, to produce H_2 or water,[31] along with the ground-state PC of Mes-Acr$^+$ regenerated.

Conclusion

In conclusion, a complementary oxidative photo-strategy assisted by *p*-NA and a visible light-induced aryltrifluoromethylation of alkenes and Langlois' reagent with hydrogen evolution to afford a range of CF_3-containing heterocycles such as indolines, indolin-2-ones, 3,4-dihydroisoquinolin-1-ones, 5,6-dihydrobenzoimidazo[2,1-*a*]isoquinolines, benzoimidazo[2,1-*a*]isoquinolin-6(5*H*)-ones and 1,2,3,4-tetrahydroisoquinolines, have been developed. This protocol is general, practical, and metal- and oxidant-free with a good functional-group tolerance. Extensive mechanistic investigations revealed that *p*-NA does not react with the PC directly as an oxidant, but rather activates HFIP via PCET and scavenges some of the reduced protons to improve proton photoreduction.

Experimental Section

General procedure for the synthesis of CF_3-containing heterocycles. A 25-mL reaction tube, equipped with a magnetic stirring bar, was charged sequentially with substrate **1**, **4**, **6**, **8**, **10**, or **12** (0.5 mmol), CF_3SO_2Na (2.0 equiv, 1.0 mmol, 156 mg), *p*-NA (1.0 equiv, 0.5 mmol, 77 mg), and Mes-Acr$^+BF_4^-$ (2 mol%, 0.01 mmol, 4 mg) under argon, followed by the addition of degassed MeCN (4.5 mL) and HFIP (0.5 mL). The mixture was stirred at room temperature under blue LED irradiation for 48 h, then it was quenched with water (20.0 mL), and extracted with CH_2Cl_2 (20.0 mL) three times. The residue obtained after evaporation of the solvent was purified by column chromatography on silica gel (petroleum ether-ethyl acetate) to afford the product. Polyfluoroalkylated small organic molecules are often volatile, and thus the solvents were removed under low-vacuum or ambient-pressure conditions.

For further experimental details including experimental procedures, spectral data, and copies of NMR and GC-MS spectra, see the Supporting Information.

Acknowledgements

We gratefully acknowledge the financial support from the Basic Research Programs of Yunnan Province (2018FH001-002, 2019FGF01/2019-1-C-25318000002188), the National Natural Science Foundation of China (22061024), the Yunnan Ten Thousand Talent Program for Young Top-Notch Talents, the Program for Innovative Research Team (in Science and Technology) in Universities of Yunnan Province, and the Undergraduate Education Reform Project of Yunnan Universities (JG2018172) and Kunming University.

Conflict of Interest

The authors declare no conflict of interest.

Keywords: photocatalysis · radical reactions · alkenes · fluorine · cyclization

[1] a) D. J. C. Constable, *ACS Sustainable Chem. Eng.* **2020**, *8*, 14657–14667; b) P. T. Anastas, J. B. Zimmerman, *Green Chem.* **2019**, *21*, 6545–6566; c) I. T. Horváth, *Chem. Rev.* **2018**, *118*, 369–371; d) K. Kümmerer, *Angew. Chem. Int. Ed.* **2017**, *56*, 16420–16421; *Angew. Chem.* **2017**, *129*, 16640–16641.
[2] a) A. Vega-Peñaloza, J. Mateos, X. Companyó, M. Escudero-Casao, L. Dell'Amico, *Angew. Chem. Int. Ed.* **2021**, *60*, 1082–1097; *Angew. Chem.* **2021**, *133*, 1096–1111; b) Y. Fang, Y. Zheng, T. Fang, Y. Chen, Y. Zhu, Q. Liang, H. Sheng, Z. Li, C. Chen, X. Wang, *Sci. China Chem.* **2020**, *63*, 149–181; c) L. Marzo, S. K. Pagire, O. Reiser, B. König, *Angew. Chem. Int. Ed.* **2018**, *57*, 10034–10072; *Angew. Chem.* **2018**, *130*, 10188–10228; d) N. A. Romero, D. A. Nicewicz, *Chem. Rev.* **2016**, *116*, 10075–10166; e) J. Xuan, W.-J. Xiao, *Angew. Chem. Int. Ed.* **2012**, *51*, 6828–6838; *Angew. Chem.* **2012**, *124*, 6934–6944.
[3] a) J. Xie, H. Jin, A. S. K. Hashmi, *Chem. Soc. Rev.* **2017**, *46*, 5193–5203; b) P. Gao, Y.-R. Gu, X.-H. Duan, *Synthesis* **2017**, *49*, 3407–3421; c) B. Peng, N. Maulide, *Chem. Eur. J.* **2013**, *19*, 13274–13287.
[4] a) H. Zhang, A. Lei, *Asian J. Org. Chem.* **2018**, *7*, 1164–1177; b) G. Zhang, C. Bian, A. Lei, *Chin. J. Catal.* **2015**, *36*, 1428–1439.
[5] a) P. Niu, J. Li, Y. Zhang, C. Huo, *Eur. J. Org. Chem.* **2020**, 5801–5814; b) X. Guo, Y. Okamoto, M. R. Schreier, T. R. Ward, O. S. Wenger, *Eur. J. Org. Chem.* **2020**, 1288–1293; c) S. Donck, A. Baroudi, L. Fensterbank, J.-P. Goddard, C. Ollivier, *Adv. Synth. Catal.* **2013**, *355*, 1477–1482.
[6] a) T. H. Meyer, I. Choi, C. Tian, L. Ackermann, *Chem* **2020**, *6*, 2484–2496; b) K. Yamamoto, M. Kuriyama, O. Onomura, *Acc. Chem. Res.* **2020**, *53*, 105–120; c) K. Sun, J. Lei, Y. Liu, B. Liu, N. Chen, *Adv. Synth. Catal.* **2020**, *362*, 3709–3726; d) P. Wang, X. Gao, P. Huang, A. Lei, *ChemCatChem* **2020**, *12*, 27–40; e) P. Xiong, H.-C. Xu, *Acc. Chem. Res.* **2019**, *52*, 3339–3350; f) Y. Yuan, A. Lei, *Acc. Chem. Res.* **2019**, *52*, 3309–3324.
[7] a) K. Dong, Q. Liu, L.-Z. Wu, *Acta Chim. Sin.* **2020**, *78*, 299–310; b) H. Wang, X. Gao, Z. Lv, T. Abdelilah, A. Lei, *Chem. Rev.* **2019**, *119*, 6769–6787; c) B. Chen, L.-Z. Wu, C.-H. Tung, *Acc. Chem. Res.* **2018**, *51*, 2512–2523; d) K.-H. He, Y. Li, *ChemSusChem* **2014**, *7*, 2788–2790.
[8] D. T. L. Alexander, P. A. Crozier, J. R. Anderson, *Science* **2008**, *321*, 833–836.
[9] For reviews, see: a) S. H. Kyne, G. Lefèvre, C. Ollivier, M. Petit, V.-A. R. Cladera, L. Fensterbank, *Chem. Soc. Rev.* **2020**, *49*, 8501–8542; b) K. C. Cartwright, A. M. Davies, J. A. Tunge, *Eur. J. Org. Chem.* **2020**, 1245–1258.
[10] For recent examples: a) J.-L. Tu, W. Tang, W. Xu, F. Liu, *J. Org. Chem.* **2021**, *86*, 2929–2940; b) J. B. McManus, J. D. Griffin, A. R. White, D. A. Nicewicz, *J. Am. Chem. Soc.* **2020**, *142*, 10325–10330; c) T. Tsukamoto, G. Dong, *Angew. Chem. Int. Ed.* **2020**, *59*, 15249–15253; *Angew. Chem.* **2020**, *132*, 15361–15365; d) H. Cao, Y. Kuang, X. Shi, K. L. Wong, B. B. Tan, J. M. C. Kwan, X. Liu, J. Wu, *Nat. Commun.* **2020**, *11*, 1956; e) Q. Xu, B. Zheng, X. Zhou, L. Pan, Q. Liu, Y. Li, *Org. Lett.* **2020**, *22*, 1692–1697.
[11] For reviews: a) J. P. Barham, B. König, *Angew. Chem. Int. Ed.* **2020**, *59*, 11732–11747; *Angew. Chem.* **2020**, *132*, 11828–11844; b) J. Liu, L. Lu, D. Wood, S. Lin, *ACS Cent. Sci.* **2020**, *6*, 1317–1340; c) Y. Yu, P. Guo, J.-S. Zhong, Y. Yuan, K.-Y. Ye, *Org. Chem. Front.* **2020**, *7*, 131–135; d) L. Capaldo, L. L. Quadri, D. Ravelli, *Angew. Chem. Int. Ed.* **2019**, *58*, 17508–17510; *Angew. Chem.* **2019**, *131*, 17670–17672.
[12] For selected examples, see: a) T. Shen, T. H. Lambert, *Science* **2021**, *371*, 620–626; b) L. Niu, C. Jiang, Y. Liang, D. Liu, F. Bu, R. Shi, H. Chen, A. D. Chowdhury, A. Lei, *J. Am. Chem. Soc.* **2020**, *142*, 17693–17702; c) N. G. W. Cowper, C. P. Chernowsky, O. P. Williams, Z. K. Wickens, *J. Am. Chem. Soc.* **2020**, *142*, 2093–2099; d) X.-L. Lai, X.-M. Shu, J. Song, H.-C. Xu, *Angew. Chem. Int. Ed.* **2020**, *59*, 10626–10632; *Angew. Chem.* **2020**, *132*, 10713–10719; e) W. Zhang, K. L. Carpenter, S. Lin, *Angew. Chem. Int. Ed.* **2020**, *59*, 409–417; *Angew. Chem.* **2020**, *132*, 417–425; f) L. Zhang, L. Liardet, J. Luo, D. Ren, M. Grätzel, X. Hu, *Nat. Catal.* **2019**, *2*, 366–373.
[13] a) M.-I. Picher, B. Plietker, *Org. Lett.* **2020**, *22*, 340–344; b) N. Lv, Y. Liu, C. Xiong, Z. Liu, Y. Zhang, *Org. Lett.* **2017**, *19*, 4640–4643.

[14] a) R. Tyburski, T. Liu, S. D. Glover, L. Hammarström, *J. Am. Chem. Soc.* **2021**, *143*, 560–576; b) J. W. Darcy, B. Koronkiewicz, G. A. Parada, J. M. Mayer, *Acc. Chem. Res.* **2018**, *51*, 2391–2399; c) N. Hoffmann, *Eur. J. Org. Chem.* **2017**, 1982–1992; d) E. C. Gentry, R. R. Knowles, *Acc. Chem. Res.* **2016**, *49*, 1546–1556.
[15] a) R. Hevey, *Chem. Eur. J.* **2021**, *27*, 2240–2253; b) Y. Ogawa, E. Tokunaga, Q. Kobayashi, K. Hirai, N. Shibata, *iScience* **2020**, *23*, 101467; c) M. Inoue, Y. Sumii, N. Shibata, *ACS Omega* **2020**, *5*, 10633–10640; d) H. Mei, A. M. Remete, Y. Zou, H. Moriwaki, S. Fustero, L. Kiss, V. A. Soloshonok, J. Han, *Chin. Chem. Lett.* **2020**, *31*, 2401–2413.
[16] a) M. Reichel, K. Karaghiosoff, *Angew. Chem. Int. Ed.* **2020**, *59*, 12268–12281; *Angew. Chem.* **2020**, *132*, 12364–12377; b) T. Koike, *Asian J. Org. Chem.* **2020**, *9*, 529–537; c) X. Pan, H. Xia, J. Wu, *Org. Chem. Front.* **2016**, *3*, 1163–1185; d) C. Alonso, E. M. de Marigorta, G. Rubiales, F. Palacios, *Chem. Rev.* **2015**, *115*, 1847–1935.
[17] a) L. Liu, D.-Y. Yang, Y.-H. He, Z. Guan, *J. Org. Chem.* **2020**, *85*, 11892–11901; b) X.-F. Xia, S.-L. Zhu, D. Wang, Y.-M. Liang, *Adv. Synth. Catal.* **2017**, *359*, 859–865; c) L. Zheng, C. Yang, Z. Xu, F. Gao, W. Xia, *J. Org. Chem.* **2015**, *80*, 5730–5736; d) C. Liu, W. Zhao, Y. Huang, H. Wang, B. Zhang, *Tetrahedron* **2015**, *71*, 4344–4351; e) X.-J. Tang, C. S. Thomoson, W. R. Dolbier Jr., *Org. Lett.* **2014**, *16*, 4594–4597.
[18] a) Z. Yang, Y. Cheng, J. Long, X. Feng, R. Tang, J. Wei, *New J. Chem.* **2019**, *43*, 18760–18766; b) Z. Yang, A. Tang, *Synlett* **2019**, *30*, 1061–1066; c) J. Zheng, R. Chen, Y. Yuan, J. Cheng, *J. Org. Chem.* **2017**, *82*, 5790–5797; d) S. Tang, Y.-L. Deng, J. Li, W.-X. Wang, G.-L. Ding, M.-W. Wang, Z.-P. Xiao, Y.-C. Wang, R.-L. Sheng, *J. Org. Chem.* **2015**, *80*, 12599–12605.
[19] a) H. Ge, B. Wu, Y. Liu, H. Wang, Q. Shen, *ACS Catal.* **2020**, *10*, 12414–12424; b) V. O. Smirnov, A. S. Maslov, V. A. Kokorekin, A. A. Korlyukov, A. D. Dilman, *Chem. Commun.* **2018**, *54*, 2236–2239; c) G. Zou, X. Wang, *Org. Biomol. Chem.* **2017**, *15*, 8748–8754.
[20] a) J. Wang, K. Sun, X. Chen, T. Chen, Y. Liu, L. Qu, Y. Zhao, B. Yu, *Org. Lett.* **2019**, *21*, 1863–1867; b) N.-Y. Yang, Z.-L. Li, L. Ye, B. Tan, X.-Y. Liu, *Chem. Commun.* **2016**, *52*, 9052–9055; c) J. Zheng, Z. Deng, Y. Zhang, S. Cui, *Adv. Synth. Catal.* **2016**, *358*, 746–751; d) G. Han, Q. Wang, L. Chen, Y. Liu, Q. Wang, *Adv. Synth. Catal.* **2016**, *358*, 561–566; e) G. Han, Y. Liu, Q. Wang, *Org. Lett.* **2014**, *16*, 3188–3191; f) W. Kong, M. Casimiro, E. Merino, C. Nevado, *J. Am. Chem. Soc.* **2013**, *135*, 14480–14483; g) W. Kong, M. Casimiro, N. Fuentes, E. Merino, C. Nevado, *Angew. Chem. Int. Ed.* **2013**, *52*, 13086–13090; *Angew. Chem.* **2013**, *125*, 13324–13328; h) P. Xu, J. Xie, Q. Xue, C. Pan, Y. Cheng, C. Zhu, *Chem. Eur. J.* **2013**, *19*, 14039–14042; i) X. Dong, R. Sang, Q. Wang, X.-Y. Tang, M. Shi, *Chem. Eur. J.* **2013**, *19*, 16910–16915.
[21] a) J. Guo, C. Xu, L. Wang, W. Huang, M. Wang, *Org. Biomol. Chem.* **2019**, *17*, 4593–4599; b) J. Guo, C. Xu, X. Liu, M. Wang, *Org. Biomol. Chem.* **2019**, *17*, 2162–2168.
[22] a) D. Liang, Q. Dong, P. Xu, Y. Dong, W. Li, Y. Ma, *J. Org. Chem.* **2018**, *83*, 11978–11986; b) M. Lu, Z. Liu, J. Zhang, Y. Tian, H. Qin, M. Huang, S. Hu, S. Cai, *Org. Biomol. Chem.* **2018**, *16*, 6564–6568; c) R. Sakamoto, H. Kashiwagi, S. Selvakumar, S. A. Moteki, K. Maruoka, *Org. Biomol. Chem.* **2016**, *14*, 6417–6421; d) L. Zhang, Z. Li, Z.-Q. Liu, *Org. Lett.* **2014**, *16*, 3688–3691; e) F. Yang, P. Klumphu, Y.-M. Liang, B. H. Lipshutz, *Chem. Commun.* **2014**, *50*, 936–938; f) L. Shi, X. Yang, Y. Wang, H. Yang, H. Fu, *Adv. Synth. Catal.* **2014**, *356*, 1021–1028.
[23] a) L. Li, M. Deng, S.-C. Zheng, Y.-P. Xiong, B. Tan, X.-Y. Liu, *Org. Lett.* **2014**, *16*, 504–507; b) J.-S. Lin, X.-G. Liu, X.-L. Zhu, B. Tan, X.-Y. Liu, *J. Org. Chem.* **2014**, *79*, 7084–7092; c) W. Fu, F. Xu, Y. Fu, C. Xu, S. Li, D. Zou, *Eur. J. Org. Chem.* **2014**, 709–712; d) Y.-F. Wang, J. Qiu, D. Kong, F.-X. Chen, *Synlett* **2014**, *25*, 1731–1734; e) X. Mu, T. Wu, H.-Y. Wang, Y.-L. Guo, G. Liu, *J. Am. Chem. Soc.* **2012**, *134*, 878–881.
[24] Examples of other CF_3 sources: a) S. Kawamura, M. Sodeoka, *Angew. Chem. Int. Ed.* **2016**, *55*, 8740–8743; *Angew. Chem.* **2016**, *128*, 8882–8885; b) J.-Y. Guo, R.-X. Wu, J.-K. Jin, S.-K. Tian, *Org. Lett.* **2016**, *18*, 3850–3853; c) S. Tang, Z.-H. Li, M.-W. Wang, Z.-P. Li, R.-L. Sheng, *Org. Biomol. Chem.* **2015**, *13*, 5285–5288.
[25] a) Z. Li, L. Jiao, Y. Sun, Z. He, Z. Wei, W.-W. Liao, *Angew. Chem. Int. Ed.* **2020**, *59*, 7266–7270; *Angew. Chem.* **2020**, *132*, 7333–7337; b) Z. Ruan, Z. Huang, Z. Xu, G. Mo, X. Tian, X.-Y. Yu, L. Ackermann, *Org. Lett.* **2019**, *21*, 1237–1240; c) Z. Zhang, L. Zhang, Y. Cao, F. Li, G. Bai, G. Liu, Y. Yang, F. Mo, *Org. Lett.* **2019**, *21*, 762–766.
[26] C. Zhang, *Adv. Synth. Catal.* **2014**, *356*, 2895–2906.
[27] K.-L. Zuo, Y.-H. He, Z. Guan, *Eur. J. Org. Chem.* **2019**, 939–948.
[28] a) W. Huang, X. Li, X. Song, Q. Luo, Y. Li, Y. Dong, D. Liang, B. Wang, *J. Org. Chem.* **2019**, *84*, 6072–6083; b) D. Liang, B. Huo, Y. Dong, Y. Wang, Y. Dong, B. Wang, Y. Ma, *Chem. Asian J.* **2019**, *14*, 1932–1936; c) Y. Li, Y. Chang, Y. Li, C. Cao, J. Yang, B. Wang, D. Liang, *Adv. Synth. Catal.* **2018**, *360*, 2488–2492; d) D. Liang, D. Ge, Y. Lv, W. Huang, B. Wang, W. Li, *J. Org. Chem.* **2018**, *83*, 4681–4691; e) D. Liang, Y. Li, S. Gao, R. Li, X. Li, B. Wang, H. Yang, *Green Chem.* **2017**, *19*, 3344–3349.
[29] a) X. Meng, H. Cheng, Y. Akiyama, Y. Hao, W. Qiao, Y. Yu, F. Zhao, S.-I. Fujita, M. Arai, *J. Catal.* **2009**, *264*, 1–10; b) M. Jorge, M. N. D. S. Cordeiro, *J. Phys. Chem. C* **2007**, *111*, 17612–17626; c) J. Bu, N. D. Lilienthal, J. E. Woods, C. E. Nohrden, K. T. Hoang, D. Truong, D. K. Smith, *J. Am. Chem. Soc.* **2005**, *127*, 6423–6429; d) G. R. Stevenson, L. Echegoyen, H. Hidalgo, *J. Phys. Chem.* **1975**, *79*, 152–154; e) J. W. Rabalais, *J. Chem. Phys.* **1972**, *57*, 960–967.
[30] M. J. Frisch, et al., *Gaussian 16*, *Revision A.03*, Gaussian, Inc., Wallingford, CT, **2016**. Complete reference is given in the Supporting Information.
[31] a) S. Doherty, J. G. Knight, T. Backhouse, R. J. Summers, E. Abood, W. Simpson, W. Paget, R. A. Bourne, T. W. Chamberlain, R. Stones, K. R. J. Lovelock, J. M. Seymour, M. A. Isaacs, C. Hardacre, H. Daly, N. H. Rees, *ACS Catal.* **2019**, *9*, 4777–4791; b) Y. Xie, X. Shang, D. Liu, H. Zhao, Y. Gu, Z. Zhang, X. Wang, *Appl. Catal. B* **2019**, *259*, 118087; c) P. Ji, K. Manna, Z. Lin, X. Feng, A. Urban, Y. Song, W. Lin, *J. Am. Chem. Soc.* **2017**, *139*, 7004–7011; d) L. J. Núñez-Vergara, S. Bollo, A. M. Atria, J. Carbajo, S. Gunckel, J. A. Squella, *J. Electrochem. Soc.* **2002**, *149*, E374–E382.

Manuscript received: February 25, 2021
Revised manuscript received: March 31, 2021
Accepted manuscript online: April 2, 2021
Version of record online: ■■, ■■■

FULL PAPERS

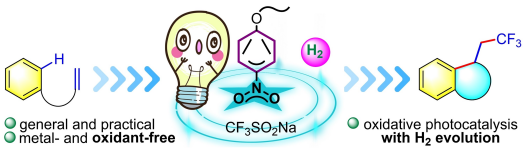

R. Kong, T. Fu, R. Yang, D. Chen, Prof. Dr. D. Liang, Dr. Y. Dong, Prof. W. Li, Prof. Dr. B. Wang*

Radical reactions: A *p*-nitroanisole (*p*-NA) assisted strategy to achieve oxidative photocatalysis with H_2 evolution is presented. Using hexafluoroisopropanol (HFIP) as a proton source and *p*-NA to activate HFIP, the proton photoreduction is enhanced, enabling a range of aryltrifluoromethylative cyclizations of alkenes and Langlois' reagent to afford various CF_3-containing heterocycles. 4-Nitroanisole facilitates proton reduction: visible light-induced oxidative aryltrifluoromethylation of alkenes with hydrogen evolution (Deqiang Liang and co-workers from Kunming University and Shandong Normal University)